Nucleon Exchange and A/Z Equilibration in Interactions of 8.3-MeV/amu ^{56}Fe Ions with ^{56}Fe, ^{165}Ho, and ^{209}Bi

H. Breuer, B. G. Glagola, and V. E. Viola
Department of Chemistry and Cyclotron Laboratory, University of Maryland, College Park, Maryland 20742

and

K. L. Wolf and A. C. Mignerey
Chemistry Division, Argonne National Laboratory, Argonne, Illinois 60439

and

J. R. Birkelund, D. Hilscher,[a] A. D. Hoover, J. R. Huizenga, W. U. Schröder, and W. W. Wilcke
Department of Chemistry and Physics and Nuclear Structure Research Laboratory, University of Rochester, Rochester, New York 14627

(Received 7 May 1979)

Yields have been measured with discrete Z and A resolution for Fe-like fragments produced in damped collisions between 8.3 MeV/amu ^{56}Fe ions and ^{56}Fe, ^{165}Ho, and ^{209}Bi targets. Both the fragment A/Z ratio and the relationship between the variances of the mass and charge distributions are found to depend upon the degree of energy damping. These observations are consistent with similar time scales for evolution of the nucleon-exchange process, A/Z equilibration, and energy dissipation.

There is considerable evidence that the major part of the energy loss in damped collisions between complex nuclei is due to dissipation mechanisms occurring on the same time scale as nucleon-exchange processes.[1] Under this condition, the variances of the product mass distributions at any value of the dissipated energy is related to the number of nucleons exchanged during the interaction time. Most previous measurements involving projectiles heavier than ^{40}Ca have determined only the charge distributions separately. However, the relation between the variances σ_N^2, σ_Z^2, and σ_A^2 of the respective neutron, charge, and mass distributions is of considerable interest since it depends on the degree of correlation[2] between neutron and proton exchange. The correlation coefficient ρ is defined by

$$\sigma_A^2 = \sigma_Z^2 + \sigma_N^2 + 2\rho\sigma_Z\sigma_N$$

with $-1 \leq \rho \leq 1$. In a classical model[2] for fully correlated neutron and proton exchange, $\rho = 1$ and $\sigma_A^2 = (A/Z)^2\sigma_Z^2$; for uncorrelated exchange, $\rho = 0$ and $\sigma_A^2 = (A/Z)\sigma_Z^2$ (where A and Z represent the combined system).

Another important feature of damped collisions is the degree of mass-to-charge equilibration of the fragments as a function of energy damping and target-projectile mass asymmetry. From inspection of the potential energy surfaces for reactions between heavy complex nuclei, as derived from the Q_{gg} systematics, one in general finds a gradient toward an equilibrium A/Z ratio which minimizes the potential energy of the composite system. Although several experiments have provided evidence in support of A/Z equilibration,[1,3-7] no data presently exist which demonstrate the detailed dependence of this equilibration process on energy loss. In order to investigate the above questions, yields of projectilelike fragments have been measured with discrete A and Z resolution as a function of energy loss for both symmetric and asymmetric systems with varying A/Z ratios.

The measurements were performed with 465-MeV ^{56}Fe ions from the Lawrence Berkeley Laboratory SuperHILAC accelerator. Self-supporting targets of monoisotopic ^{56}Fe, ^{165}Ho, and ^{209}Bi with thicknesses of approximately 500 μg/cm^2 were used. The projectilelike fragments were detected with a time-of-flight ΔE-E telescope consisting of 17-μm ΔE and 100-μm E silicon surface-barrier detectors. Data were taken at selected angles forward of the grazing angles. The separation distance between the ΔE and E detectors was 100 cm and timing signals were derived from Sherman-Roddick fast-timing electronics.[8] For elastically scattered ^{56}Fe ions a timing resolution of 100 psec and an energy resolution of approximately 3 MeV were obtained, resulting in a mass resolution of ≈ 0.7 amu. The ΔE-E signals provided Z resolution of ≤ 0.8 charge units, thus permitting discrete Z and A identification for all Fe-like products. In Fig. 1 a two-dimensional plot of experimental yields for the ^{209}Bi + ^{56}Fe bombardment is shown.

Since the data represent the yields of residual

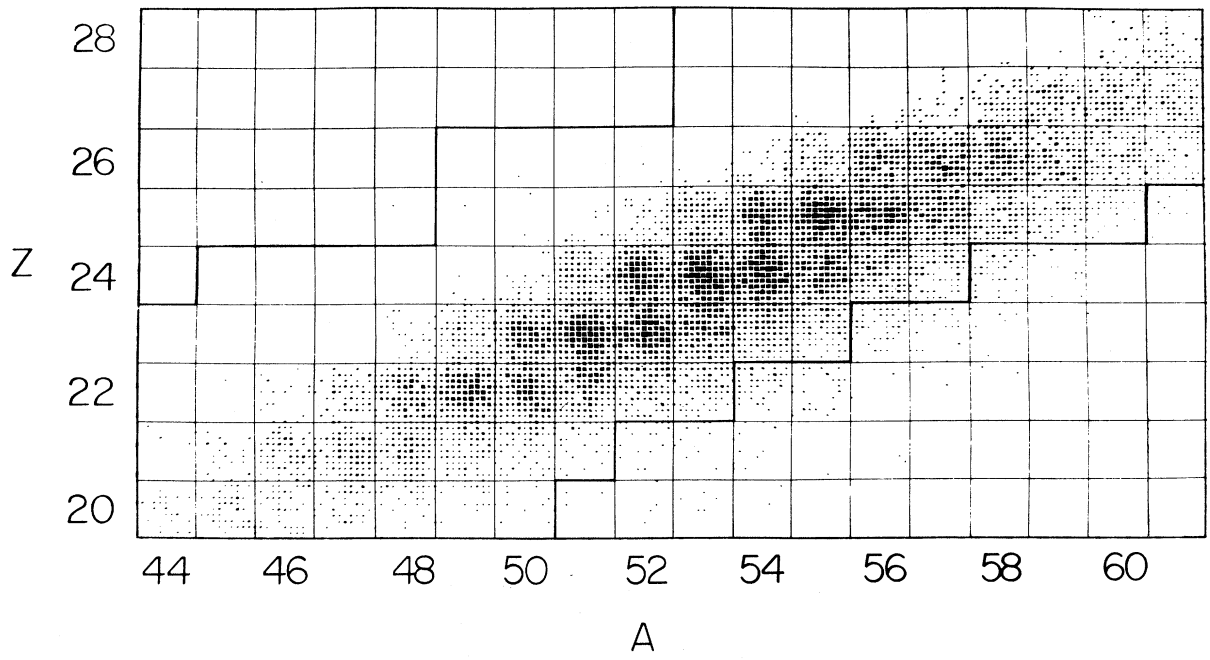

FIG. 1. Plot of charge vs mass for the Bi + Fe reaction at $60 \leq E_{\text{loss}} \leq 160$ MeV. The sizes of the points correspond to counts on a quadratic scale. The region of currently known particle-stable nuclei falls between the limits indicated by the intensified solid lines.

Fe-like fragments after deexcitation, it is necessary to correct for particle evaporation in order to obtain primary yields. The available excitation energy is assumed to be shared between the two primary products according to their mass ratio. Neutron multiplicity and energy measurements support this assumption for Ho + Fe system.[7] Using nucleon binding energies from the compilation of Wapstra and Bos[9] and treating the energy spectra of the emitted particles as described in Ref. 7, the measured yields and energies were transformed by an iterative, event-by-event procedure into primary fragment yields and center-of-mass energies. These calculations indicate that neutron evaporation predominates over charged-particle emission for the Ho + Fe and Bi + Fe cases due to the neutron excess and relatively low excitation energies of the primary Fe-like fragments. Hence, the measured charge distributions for these two heavier systems can be considered to be essentially primary yields. However, in the Fe + Fe system greater proton richness and higher excitation energies increase the relative importance of charged-particle emission. These conclusions are corroborated by measurements of charged-particle emission performed simultaneously in these experiments. While particle emission gives measured average mass of the primary fragments, the effect on the variances of the mass distributions is small. Neutron evaporation leads to measured mass distributions which are narrower than the primary distributions, whereas proton evaporation produces the opposite effect. Thus the primary variances of the mass distributions for the Fe + Fe reaction fragments are essentially the same as those of the measured distributions.

Figure 2 presents the experimental results as a function of total kinetic energy loss (E_{loss}). The data points on the left-hand side of the plot represent the shifts of the average mass, $\Delta\bar{A} = \bar{A} - 56$, whereas on the right-hand side the variances of the mass distributions, σ_A^2, are plotted. Triangles indicate measured data points and circles show values of $\Delta\bar{A}$ and σA^2 corrected for neutron emission. The curves represent the corresponding measured values of $\Delta\bar{Z} = \bar{Z} - 26$ and σ_Z^2, multiplied by A/Z of the composite systems (dashed lines) and $(A/Z)^2$ (solid lines), respectively, for comparison with the mass data. Values for $\bar{Z}$, $\bar{A}$, σ_A^2, and σ_Z^2 were obtained from Gaussian fits to the data.

First, the implications of these data on the charge-equilibration mechanism are discussed.

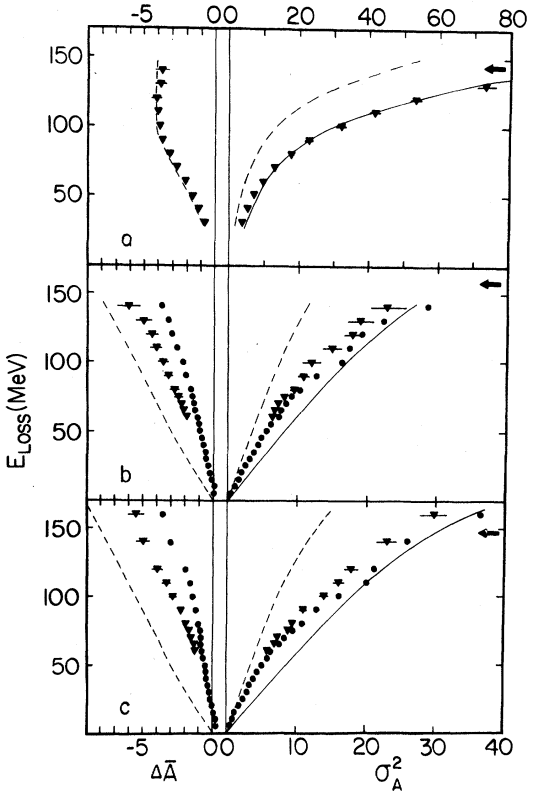

FIG. 2. Values of $\Delta\bar{A}$ (left-hand sides) and variances of the mass distributions (right-hand sides) as a function of energy loss for the reactions of ^{56}Fe ions with (a) ^{56}Fe at 8°; (b) ^{165}Ho at 30°; and (c) ^{209}Bi at 34° and 38° in the laboratory system. Note the change in scale for σ^2 for the Fe + Fe reaction. Arrows indicate the respective Coulomb barriers for touching spheres in the entrance channels. Triangles give measured points with statistical errors; circles represent the data corrected for neutron emission (errors are comparable to measured points). The dashed lines show the values of $\Delta\bar{Z} = 26 - \bar{Z}$ and σ_Z^2 multiplied by (A/Z); the solid line represents σ_Z^2 times $(A/Z)^2$.

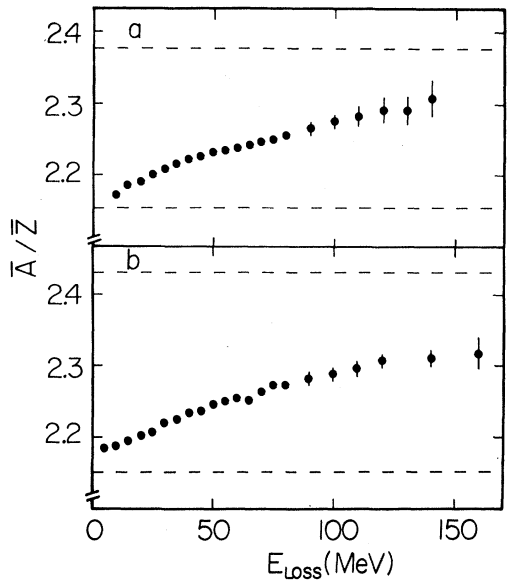

FIG. 3. Ratios of $\bar{A}/\bar{Z}$, corrected for neutron evaporation, as a function of energy loss for the (a) ^{165}Ho and (b) ^{209}Bi + ^{56}Fe systems. The dashed lines give A/Z of the projectile and of the composite systems.

For all three systems the data exhibit a drift of $\bar{Z}$ toward smaller atomic numbers as the energy damping increases. For the Fe + Fe system this drift is attributed to charged-particle emission in the deexcitation of the primary fragments. Since for the Ho + Fe and Bi + Fe systems charged-particle emission is strongly inhibited, their decrease in $\bar{Z}$ must be attributed to a charge-equilibration process in which protons are preferentially transferred from the Fe-like fragments to the heavy partner.

From the measured values of Z and A, corrected for neutron evaporation for the two heavier systems, it is possible to deduce the dependence of $\bar{A}/\bar{Z}$ on E_{loss}, as shown in Fig. 3. Also shown as dashed lines are the A/Z ratios of the ^{56}Fe projectile (2.15) and of the composite systems (2.38 for Ho + Fe and 2.43 for Bi + Fe). The data support a nucleon-exchange mechanism in which there is an initial increase in the $\bar{A}/\bar{Z}$ value of the primary Fe-like fragments as soon as the Q values permit. Thereafter a monotonic increase in $\bar{A}/\bar{Z}$ is observed which may saturate at energy losses in the range of 100–150 MeV at $\bar{A}/\bar{Z} \approx 2.3$ for both asymmetric systems. These values are close to the equilibrium values defined by potential energy surfaces based on the liquid-drop model including shell corrections, which are somewhat smaller than the $\bar{A}/\bar{Z}$ of the combined systems.

The measured variances of the mass and charge distributions are compared on the right-hand side of Fig. 2. Neither assumption of correlated or uncorrelated diffusion (dashed lines) describe the variances of the mass distributions for any of the systems studied in this work. Instead, a behavior intermediate between uncorrelated and correlated exchange is observed for partially damped events, but with increasing energy loss all three systems evolve toward correlated exchange (consistent with the square of the observed $\bar{A}/\bar{Z}$ ratio). This aspect of the data is demonstrated more explicitly in Fig. 4 where the dependence of σ_A^2/σ_Z^2 on energy loss is plotted. For com-

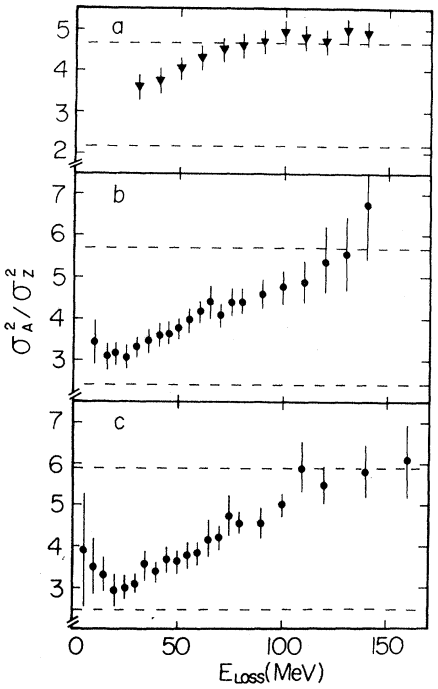

FIG. 4. Ratios of σ_A^2/σ_Z^2 as a function of energy loss for the (a) ^{56}Fe, (b) ^{165}Ho, and (c) ^{209}Bi + ^{56}Fe systems. Data points in (a) (triangles) represent the measured values, in (b) and (c) (circles) values corrected for neutron evaporation. The dashed lines represent A/Z and $(A/Z)^2$ of the composite system.

parison the upper and lower dashed lines represent the A/Z and $(A/Z)^2$ values of the combined system, respectively. It is noted in Fig. 4 that the limit of correlated exchange is reached for the Fe + Fe system at about half the energy loss of the two asymmetric systems. Previous studies of the ^{168}Er + ^{86}Kr system[6] at energy losses greater than 100 MeV have shown similar agreement with the relation $\sigma_A^2 = (A/Z)^2\sigma_Z^2$. However, the present data stress the importance of the degree of energy damping in reaching the correlated limit.

In summary, charge and mass distributions have been measured for the products formed in damped collision processes in three heavy-ion systems of widely differing target-projectile mass asymmetries and A/Z values. The excellent resolution for Z and A permits the determination of precise values for $\bar{A}$, $\bar{Z}$, σ_Z^2, and σ_A^2. The $\bar{Z}$ and $\bar{A}$ results show that charge equilibration develops gradually with increasing energy loss. Hence, for very asymmetric systems, an equilibrium in A/Z is not achieved until the reaction is almost totally damped, requiring comparatively long interaction times. The relationship between σ_Z^2 and σ_A^2 supports a correlated-nucleon diffusion mechanism for interaction times sufficiently long that the limiting $\bar{A}/\bar{Z}$ value has been reached. This is consistent with time scales for evolution of the correlations in the nucleon exchange, the equilibration of A/Z, and the energy dissipation. The energy-loss time scale leads to an interaction time of $(4-8)\times10^{-22}$ sec at 100 MeV energy loss for the nonsticking and sticking conditions,[1,7] at which time the correlations in nucleon exchange and A/Z ratio seem to be close to steady-state values.

This work was supported by the U. S. Department of Energy. We wish to thank Dr. M. S. Zisman for his assistance with these experiments and the staff of the Lawrence Berkeley Laboratory SuperHILAC for providing the beams. One of us (V.E.V.) thanks the University of Maryland for providing a University Research Professorship during the time this work was being carried on.

[a]On leave of absence from the Hahn-Meitner Institut, Berlin, West Germany.

[1]W. U. Schröder and J. R. Huizenga, Annu. Rev. Nucl. Sci. 27, 465 (1977).

[2]F. Beck, M. Dworzecka, and H. Feldmeier, Z. Phys. A 289, 113 (1978).

[3]B. Gatty *et al.*, Nucl. Phys. A253, 511 (1975).

[4]J. V. Kratz *et al.*, Phys. Rev. Lett. 39, 984 (1977).

[5]J. Barrette *et al.*, Nucl. Phys. A299, 147 (1978); P. Braun-Munzinger and J. Barrette, Nucl. Phys. A299, 161 (1978).

[6]Y. Eyal, G. Rudolf, I. Rode, and H. Stelzer, Phys. Rev. Lett. 42, 826 (1979).

[7]D. Hilscher *et al.*, Phys. Rev. C (to be published).

[8]I. S. Sherman, R. G. Roddick, and A. F. Metz, IEEE Trans. Nucl. Sci. 15, 500 (1968).

[9]A. H. Wapstra and K. Bos, At. Data Nucl. Data Tables 19, 177 (1977).